ELSEVIER International Journal of Mass Spectrometry and Ion Processes 148 (1995) 203–213

International Journal of Mass Spectrometry and Ion Processes

Electron-impact ionization of ozone

Karl A. Newson[a], Stephanie M. Luc[a], Stephen D. Price[a,*], Nigel J. Mason[b]

[a]*Chemistry Department, University College London, Christopher Ingold Laboratories, 20 Gordon Street, London, WC1H 0AJ UK*
[b]*Department of Physics and Astronomy, University College London, Gower Street, London WC1E 6BT UK*

Received 6 June 1995; accepted 21 July 1995

Abstract

Partial electron ionization cross-sections of ozone for incident electron energies from 40 to 500 eV have been determined using time-of-flight mass spectrometry. The cross-sections are derived by identifying the contribution of ozone to the ion signals recorded following ionization of a mixture of O_2 and O_3. Only one previous determination of these cross-sections, for energies up to 100 eV, is available in the literature. The cross-sections derived in the present study at these lower electron energies are in good agreement with the previous determination.

Keywords: Electron ionization; Ozone; Partial ionization cross-sections; Time-of-flight mass spectrometry

1. Introduction

Ozone is an important agent in the chemistry of the stratosphere, where it absorbs much of the biologically harmful UV radiation that would otherwise reach the Earth's surface. The recognition of the importance of ozone in controlling the Earth's thermal and radiation budget has led to extensive studies of the physics and chemistry of ozone [1,2]. From the viewpoint of collision dynamics, the asymmetric polar molecule O_3 presents a severe test for theoretical models of electron/molecule scattering [3–5]. However, at present there are few experimental studies of the collision dynamics of ozone for comparison with theory [6,7]. In fact, only one determination of the electron impact partial ionization cross-sections of ozone has been reported, the data covering a restricted energy range up to 100 eV [8].

Mass spectrometric experiments aiming to study quantitatively the ionization of ozone face a serious difficulty in that ozone is an extremely reactive molecule and will rapidly decompose when in contact with many metallic and non-metallic surfaces [2,9]. Hence, any sample of ozone introduced into a mass spectrometer may easily be degraded, and a mixture of O_3 and O_2 in the ionization source will result. Previous experimental studies indicate that this in situ degradation may exceed 10% of the O_3 present [10]. Hence, one cannot assign directly all the O_2^+ and O^+ signals detected mass spectrometrically following the ionization of a sample of ozone to purely the fragmentation of O_3^+; it is also necessary to

* Corresponding author.

SSDI 0168-1176(95)04300-4

determine those contributions arising from the O_2 that may be present.

The only previous determination of the electron ionization cross-sections of ozone employed a modulated-beam quadrupole mass spectrometer [8]. This experimental technique involves the ionization of a chopped gas beam, and in principle allows the separation of the fragment ion signals from ionization of O_2 and O_3 by their phase shift relative to the modulation frequency. The ozone sample in these earlier experiments was introduced by a short, all-glass inlet system, from a sample of O_3 cooled by liquid oxygen. Using this arrangement, the analysis of the phase shifts in the mass spectra indicated that, within the experimental error limits, all the oxygen-containing ions observed were due to the ionization of O_3.

As part of a series of studies of electron scattering from aeronomic species, this paper presents a determination of the partial electron ionization cross-sections of ozone over an extended energy range from 40 to 500 eV using time-of-flight mass spectrometry. The problems of in situ ozone decomposition, which are found to be non-negligible, are overcome by using the existing cross-sections at 100 eV to determine the composition of the O_3/O_2 mixture in the ionization source.

2. Experimental

In this investigation, the partial electron ionization cross-sections of ozone have been derived from mass spectra recorded at electron energies from 40 to 500 eV using a time-of-flight mass spectrometer. The time-of-flight mass spectrometer is illustrated schematically in Fig. 1. It is a two-field device, constructed to the standard Wiley–McLaren design [11], with a first-order space focus. An effusive jet of target gas and an electron beam generated from a modified VG electron gun enter the source region of the mass spectrometer via stainless steel needles and intersect perpendicularly in the centre of the source. The current emitted from the filament is monitored at a lens element situated before the needle which transports the beam into the ion source (Fig. 1). Experiments were performed with an incident current of 10 μA reaching this lens, and under these conditions an electron current of less than 0.5 nA passes down the needle and crosses the interaction region. The energy of the electron beam was calibrated by a determination of the ionization thresholds of the rare gases. These same experiments indicate that the energy spread of the electron beam was ± 2 eV. A mass spectrum is recorded by pulsing the repeller plate (Fig. 1) of the ion source to a positive voltage (+200 V) and recording the arrival times of positive ions at the channeltron detector using a multi-channel scalar (EG&G Turbo-MCS). An extraction pulse width of 10 μs was employed with a period of 50 μs. When the electric field is applied, the electron beam is markedly deflected and no longer intersects the gas beam in the region of space from which ions are imaged onto the detector. Thus, the mass spectrometer effectively operates in the conventional pulse electron beam mode previously used for studies of electron impact ionization [12]. However, problems can be encountered with such systems due to the trapping of ions with low translational energy within the space-charge of the electron beam [13]. In these circumstances, only those energetic ions formed from fragmentation processes have enough kinetic energy to escape the localized potential well of the electron beam, and the signal intensities of these species in the resulting mass spectra are markedly reduced with respect to those from ions with low translational energies which are trapped by the electron beam. In this experiment, a small voltage (−15 V) was applied to the repeller plate in between the +200 V extraction pulses. The electric field

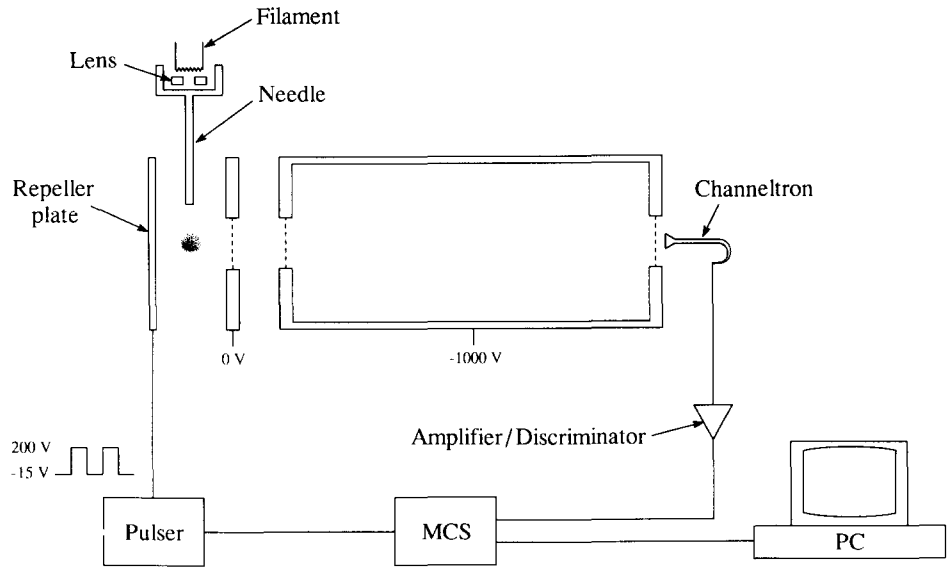

Fig. 1. Schematic diagram of the time-of-flight mass spectrometer. The gas inlet is perpendicular to the plane of the figure and is not shown.

present as a result of this −15 V bias voltage overcomes the electrostatic attraction of the electron beam, and accelerates the ions formed towards the repeller plate and out of the interaction region. If the pulse width is long enough to allow all the ions formed to exit the source and the inter-pulse period is long enough for the electron beam to re-establish its central position, the intensities of the ion signals in the mass spectra are insensitive to variations of the +200 V extraction pulse width and its duty cycle. This observation indicates that trapping effects have been eliminated as, if trapping were occurring, the relative intensities of low kinetic energy ions would increase with the interpulse period. Indeed, precisely this phenomenon is observed in the mass spectra when the −15 V bias is not present. In addition, the relative intensities of the ion signals in the mass spectra are insensitive to variations in the electron beam current. If trapping effects were significant, a significant change in the relative intensities of the ion signals with electron beam current should be observed. Under these conditions, and following the data analysis procedures described below, the mass spectra obtained from the instrument yield relative partial ionization cross-sections of argon, CS_2 and N_2O in good agreement with those available in the literature, confirming that trapping effects have been eliminated.

The ozone sample for these experiments was produced using a Fischer 502 ozonizer, which generates a silent electric discharge in a flow of dry oxygen [2,10]. The ozonized gas leaving the discharge contains only a few per cent of ozone, but trapping the ozone on silica gel at 195 K and pumping away the excess oxygen allows a gas mixture (of O_2 and O_3) with a higher mole fraction of ozone to be prepared. Such a mixture was desorbed into a 5 l bulb, suitably protected against explosion, to allow storage for subsequent experiments.

As has been established by earlier work [2,10], to obtain gas mixtures with a high mole fraction of $O_2(> 0.5)$ by the above procedure, we found it necessary to condition the gas lines handling the ozone by exposing them to an ozonized oxygen mixture for several hours prior to trapping the ozone on 6-15 mesh silica gel. Using this methodology, O_2/O_3 gas mixtures with ozone mole fractions of

about 0.8 were routinely generated. The composition of the ozone/oxygen mixture was determined mass spectrometrically, as described in the data analysis section below.

The ozone was bled into the time-of-flight mass spectrometer via a valved gas line constructed of stainless steel, glass and PTFE. To minimize the in situ degradation of the O_3 sample during a series of measurements the inlet was conditioned by prolonged exposure to ozone before any mass spectra were recorded. Typical operating pressures in the mass spectrometer, as recorded by an ion gauge, were of the order of 5×10^{-7} mmHg. In this pressure regime the signal intensities in the ozone mass spectrum were found to vary linearly with pressure, indicating that any effects due to bimolecular collisions were negligible.

3. Data analysis

Fig. 2 shows a typical mass spectrum recorded for an ozonized oxygen mixture. The analysis procedure described below indicates that this mixture has an ozone mole fraction of 0.71. It should be noted that the bias electric field, which gives the ions a significant velocity component across the interaction region results in a slight asymmetry of the ion signals. The raw data for the analysis procedure consist of the intensities of the ion signals in such mass spectra, for example $I_{O_3^+}(E)$, recorded at a range of electron energies from 40 to 500 eV. These intensities are determined by integrating the O^+, O_2^+ and O_3^+ peaks and applying a suitable background correction.

To derive the relative partial ionization cross-sections from these ion intensities it is necessary to consider the factors affecting their magnitudes. The intensity of a signal I in the mass spectrum after P pulses of the repeller plate can be expressed as

$$I_{Y^+} = \alpha(m_{Y^+})N_{Y^+} + VP \quad (1)$$

where N_{Y^+} is the number density of the ion Y^+ in the volume V of the source region that is imaged onto the detector, and $\alpha(m_{Y^+})$ is the experimental collection efficiency for ions of mass-to-charge ratio m_{Y^+}.

If σ_X is the partial ionization cross-section for forming Y^+ from the neutral molecule X, then by definition we have

$$R_{Y^+} = R_e^0 N_X \sigma_X l \quad (2)$$

where R_{Y^+} is the rate of formation of Y^+ in the interaction region and R_e^0 is the number of electrons per second entering the interaction region which has electron path length l.

Due to the presence of the bias field across the source region during the period between the +200 V extraction pulses, the ions formed have a non-zero velocity towards the repeller plate from the instant of their generation. Hence, ions of two different masses with the same partial ionization cross-section for their formation, will have different number densities in the imaged volume, due to their differing velocities across it. However, since the residence time of an ion in the source region is very small ($< 1\,\mu$s) in comparison to the inter-pulse period during which ionization is occurring, and the rate of ionization is low, the fluxes of these two species across the imaged volume will be the same. That is, after an induction period of less than $1\,\mu$s, which is the time it takes for the first ions formed to leave the interaction region, the number of the two species leaving the interaction region per unit time interval will be the same although they leave with different velocities.

If the cross-sectional area of the imaged volume perpendicular to the bias electric field is A, then the flux of Y^+ across the imaged volume is J_{Y^+} where $J_{Y^+} = R_{Y^+}/A$. At any point, $N_{Y^+} = J_{Y^+}/v_{Y^+}$, where v_{Y^+} is the velocity of Y. Since the ions are undergoing a constant acceleration across the imaged volume under the influence of the bias electric field, $v_{Y^+} = k/\sqrt{m_{Y^+}}$, where k is a constant

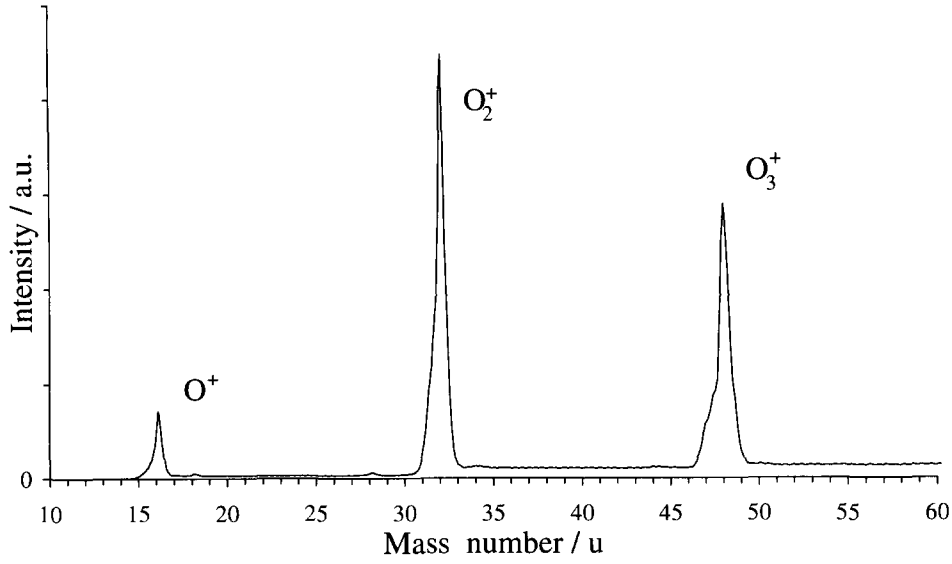

Fig. 2. A mass spectrum of a typical ozonized oxygen mixture used in this study.

depending on the position of Y^+ in the bias field. Combining these expressions gives

$$I_{Y^+} = \frac{\alpha(m_{Y^+})VPR_e^0 N_X \sigma_X l\sqrt{m_{Y^+}}}{Ak} \quad (3)$$

Modelling the ionic motions in the source region using a Monte Carlo computer simulation confirms that, under the general experimental conditions described above, ions formed at the same rate will have densities proportional to the square root of their mass, as predicted by Eq. (3). The above analysis can be tested by examining the relative intensities of the signals corresponding to single and double ionization of argon in time-of-flight mass spectra recorded on our instrument. For these spectra, using Eq. (3) we derive

$$\frac{I_{Ar^+}}{I_{Ar^{2+}}} = \frac{\sqrt{2}\alpha\sigma_{Ar^+}}{\alpha\sigma_{Ar^{2+}}} = \frac{\sqrt{2}\sigma_{Ar^+}}{\sigma_{Ar^{2+}}} \quad (4)$$

assuming the collection efficiency α for the singly and doubly charged ions is equal. The intensity ratios in our mass spectral data, transformed using Eq. (4), yield a ratio of partial ionization cross-sections in close agreement with the literature [13], confirming the above analysis.

As has been discussed in the literature [13], measuring absolute partial ionization cross-sections using a mass spectrometer is difficult, as it is necessary to determine accurate values for the experimental parameters of Eq (3). To circumvent these problems, which are exacerbated by the fact that our target gas is a mixture of ozone and oxygen of unknown and potentially varying composition, we must measure relative ion intensities and normalize the relative partial ionization cross-sections derived from these values to an absolute scale.

Given the efforts made to ensure no trapping effects are present in the spectra recorded from our time-of-flight mass spectrometer, the principal factor for causing any variations in the collection efficiency for different ions is their kinetic energy. These effects arise as ions formed with significant kinetic energies perpendicular to the axis of the mass spectrometer can move far enough away from this axis during their flight to miss the channeltron detector. Considering our experimental

geometry, and assuming a point ion source, the number of ions missing the channeltron detector will become significant for species with an initial transverse kinetic energy of greater than about 0.3 eV. This limit is determined by considering both the geometry of the mass spectrometer and allowing for the electrostatic effects of the voltage on the front of the channeltron. Hence, the mass spectrometer collects ions with initial kinetic energies below about 0.3 eV with equal efficiency, but higher energy fragment ions will be detected with a lower and steadily decreasing efficiency.

Such energy-dependent collection efficiencies have been shown to influence strongly the values of the molecular partial ionization cross-sections derived from mass spectra [14]. To evaluate their influence on the mass spectra recorded in this study we must consider the kinetic energies and origins of the ions detected. Firstly, we have parent ions, O_2^+ from O_2 and O_3^+ from O_3. These ions will have thermal velocities in the ion source and will suffer no significant losses on their flight to the detector. These thermal ions will be detected with an efficiency α depending on the efficiency of the channeltron and associated detection electronics. Secondly, we have fragment ions from the dissociation of O_3^+. Studies of the kinetic energy release distributions of triatomic parent ions, formed by electron impact, indicate that only a very small percentage of the fragment ions from these species would be expected to have kinetic energies greater than 0.3 eV [15]. So, we expect to detect fragment ions from the single ionization of ozone, and other triatomic and larger species, with an efficiency α, the same as that for thermal ions. This hypothesis was confirmed by studying the ionization of the triatomic molecules N_2O and CS_2. The ratios of the intensities of fragment to parent ions from these mass spectra, when corrected by the appropriate mass factors (as in Eq. (4)), yield ratios of the various partial ionization cross-sections in good agreement with literature values [16,17], confirming that the fragment ions from triatomic molecules are detected in our apparatus with effectively the same efficiency as thermal ions. Of course, as will be discussed in more detail below, our experimental arrangement discriminates quite strongly against singly charged ions formed by the fragmentation of multiply charged ions, as such fragments are usually formed with kinetic energies in excess of 2 eV [18].

Finally, in addition to the thermal ions and the fragment ions from the ionization ozone, our mass spectra contain signals due to O^+ ions formed following the ionization of O_2. In general, the ionic fragments from diatomic molecules possess significantly more kinetic energy than those from polyatomic species [19]. Hence, for our apparatus the collection efficiencies for such ions will be smaller than α and must be determined experimentally as described below.

Two analysis procedures are employed to evaluate the relative partial ionization cross-sections of ozone from the mass spectral ion intensities: the first to derive $\sigma^S_{O_3}$, the cross-section for producing stable O_3^+ ions, and the second to derive the dissociative ionization cross-sections, $\sigma^{D'}_{O_3}$ and $\sigma^{D''}_{O_3}$, for forming O_2^+ and O^+ respectively.

To determine $\sigma^S_{O_3}$, mass spectra are recorded with a small amount of N_2 present in the ozonized gas mixture. Using the mass spectral intensities (Eq. (3)) of the N_2^+ and O_3^+ signals at 100 eV we can then use the literature values of the stable ionization cross-sections [8,20,21] at this energy to determine a value for R, the relative number density of O_3 and N_2 in the ionization source scaled by the appropriate mass factors:

$$\frac{\sqrt{m_{O_3}}N_{O_3}}{\sqrt{m_{N_2}}N_{N_2}} = \frac{I_{O_3^+}(100)\sigma^S_{N_2}(100)}{I_{N_2^+}(100)\sigma^S_{O_3}(100)} = R \qquad (5)$$

For the intensity ratio of O_3 and N_2 at any other electron energy we therefore have

$$\frac{I_{N_2^+}(E)}{I_{O_3^+}(E)} = \frac{N_{N_2}\sqrt{m_{N_2}}\sigma^S_{N_2}(E)}{N_{O_3}\sqrt{m_{O_3}}\sigma^S_{O_3}(E)}$$

Thus,

$$\sigma^S_{O_3}(E) = \sigma^S_{N_2}(E)\frac{I_{O_3^+}(E)}{I_{N_2^+}(E)}R \tag{6}$$

This allows $\sigma^S_{O_3}$ to be determined from the mass spectral intensity ratio $I_{N_2^+}/I_{O_3^+}$ at the electron energy of interest, the literature value of the stable ionization cross-section [20,21] of N_2 at that energy and R derived from a calibration spectrum at 100 eV electron energy. Due to the slow degradation of the ozone sample in the gas bulb (usually at a rate of about 1% per day) and the in situ degradation due to the surfaces of the inlet system, frequent calibration spectra must be recorded at 100 eV. To minimize the experimental uncertainties introduced by this degradation, the value of R used to derive $\sigma^S_{O_3}$ from a given mass spectrum was taken as the average of the values from calibration spectra recorded immediately before and after the measurement.

To determine the dissociative ionization cross-sections, a series of mass spectra of an ozonized oxygen mixture rich in O_3 was recorded as a function of electron energy. In these spectra, the ionization of both O_2 and O_3 can contribute to the O_2^+ and O^+ signals observed. From Eq. (3) it follows that

$$\frac{I_{O_2^+}(E)}{I_{O_3^+}(E)} = \frac{\sqrt{m_{O_2}}[N_{O_2}(E) + N_{O_3}\sigma^{D'}_{O_3}(E)]}{N_{O_3}\sqrt{m_{O_3}}\sigma^S_{O_3}(E)} \tag{7}$$

If we define a composition parameter x such that $N_{O_3} = xN$, where N is the total number density of neutral molecules (O_2 and O_3) in the source region, then $N_{O_2} = (1-x)N$ and

$$x = \left[\frac{\sqrt{m_{O_3}}I_{O_2^+}(E)\sigma^S_{O_3}}{\sqrt{m_{O_2}}I_{O_3^+}(E)\sigma^S_{O_2}(E)} - \frac{\sigma^{D'}_{O_3}(E)}{\sigma^S_{O_2}(E)} + 1\right]^{-1} \tag{8}$$

From a mass spectrum at 100 eV, and the literature values of $\sigma^S_{O_2}$, $\sigma^{D'}_{O_3}$ at that electron energy [8,22] we can therefore determine the value of x, the mole fraction of ozone for the sample in the source. This procedure indicates that we routinely generate gas mixtures with an O_3 mole fraction greater than 0.70 in the interaction region of the ion source. In fact, the relative ozone mole fraction in the gas bulb will be greater than this value due to degradation effects in the gas line and effusive effects [12] in the gas needle admitting the sample to the mass specrometer. To check the validity of this procedure, we performed a mass spectrometric determination of the composition of a sample of ozonized oxygen for which the ozone composition in the gas bulb and has been determined spectroscopically [23]. The value of x derived from the mass spectrum (72%) was perfectly consistent with the spectroscopic value derived for the gas in the bulb (75%).

Using the value of x derived at 100 eV, the mass spectral intensity ratio at other electron energies, the stable ionization cross-section of O_3 derived above and the literature values of the stable ionization cross-section [22] of O_2, we can then determine $\sigma^{D'}_{O_3}(E)$:

$$\sigma^{D'}_{O_3}(E) = \frac{\sqrt{m_{O_3}}I_{O_2}(E)\sigma^S_{O_3}}{\sqrt{m_{O_2}}I_{O_3}(E)} - \frac{\sigma^S_{O_2}(E)}{x} + \sigma^S_{O_2}(E) \tag{9}$$

A similar procedure is used to determine $\sigma^{D''}_{O_3}(E)$ from the same series of mass spectra. In this case we must allow for the fact that the O^+ ions from O_2^+ are formed with a considerable kinetic energy and are detected with less than our standard collection efficiency α. If the

detection efficiency of these energetic O^+ ions is α', then we have

$$\frac{I_{O^+}(E)}{I_{O_3^+}(E)} = \frac{\sqrt{m_O}(\alpha x \sigma^{D''}_{O_3}(E) + \alpha'(1-x)\sigma^{D}_{O_2}(E))}{\alpha\sqrt{m_{O_3}} x \sigma^{S}_{O_3}(E)} \tag{10}$$

$$\sigma^{D''}_{O_3}(E) = \frac{\sqrt{m_{O_3}} I_{O^+}(E)\sigma^{S}_{O_3}(E)}{\sqrt{m_O} I_{O_3^+}(E)} - \frac{\alpha'\sigma^{D}_{O_2}(E)}{\alpha x} + \frac{\alpha'\sigma^{D}_{O_2}(E)}{\alpha} \tag{11}$$

At a given electron energy, we can determine the terms involving α' in Eq. (11), which represent the contribution to the O^+ signal from the dissociation of O_2, from the intensity ratio of O^+ to O_2^+ $[I_O(E,O_2)/I_{O_2}(E,O_2)]$ in a mass spectrum of pure O_2. For this pure oxygen spectrum we have

$$\frac{I_{O^+}(E,O_2)}{I_{O_2^+}(E,O_2)} = \frac{\alpha'\sqrt{m_O}\sigma^{D}_{O_2}(E)}{\sigma\sqrt{m_{O_2}}\sigma^{S}_{O_2}(E)} \tag{12}$$

$$\therefore \frac{\alpha'\sigma^{D}_{O_2}(E)}{\alpha} = \frac{\sqrt{m_{O_2}}\sigma^{S}_{O_2}(E)}{\sqrt{m_O}} \frac{I_{O^+}(E,O_2)}{I_{O_2^+}(E,O_2)} \tag{13}$$

The expression involving α' (Eq. (13)) is determined, as a function of the electron energy, from the intensity ratio in the O_2 mass spectrum, and the literature values [22] of $\sigma^{S}_{O_2}$ can be substituted directly into Eq. (11) which together with the appropriate value of x and the O_3^+ to O^+ intensity ratio from the mass spectrum of the ozonized oxygen mixture, yields $\sigma^{D''}_{O_3}(E)$.

4. Results

Partial ionization cross-sections derived by the procedure outlined above, at incident electron energies from 40 to 500 eV, are shown in Fig. 3 and listed in Table 1. These values are the average of at least six independent determinations. The standard deviations between the six values at each electron energy are shown in Table 1, and are low in accord with the small statistical error in each of the determinations (about 8%). No estimates of the error limits for the ozone partial ionization cross-sections at 100 eV which we use in our data analysis are available. Hence, our estimate of the error in a single determination of one cross-section is made by considering only the counting statistics in the mass spectra. However, as has been discussed before [13], systematic errors and the typical uncertainties in the literature values for molecular partial ionization cross-sections probably result in an overall error bar of ±15% for experimental determinations of molecular partial ionization cross-sections.

5. Discussions

As shown in Fig. 3, the values of the partial ionization cross-sections for ozone determined in this work at electron energies below 100 eV are in good agreement with the only previous study reported in the literature [8]. To our knowledge the values above 100 eV presented in this work are the first to be reported. The cross-sections for the stable ionization of O_3 determined in this work below 100 eV are slightly lower (5–10%) than the previously reported values; however, these deviations lie within the error limits discussed above. The agreement at 100 eV is a result of the normalization procedure. As shown in Fig. 3, the cross-sections derived for the formation of O_2^+ from O_3 below 100 eV incident electron energy agree very well with the only previous determination. Again the data analysis procedure, which is described above, produces the agreement observed at 100 eV. The dip in the cross-section curve (Fig. 3(b)) at 450 eV incident electron energy appears to be a real feature. Repeated determinations of this and

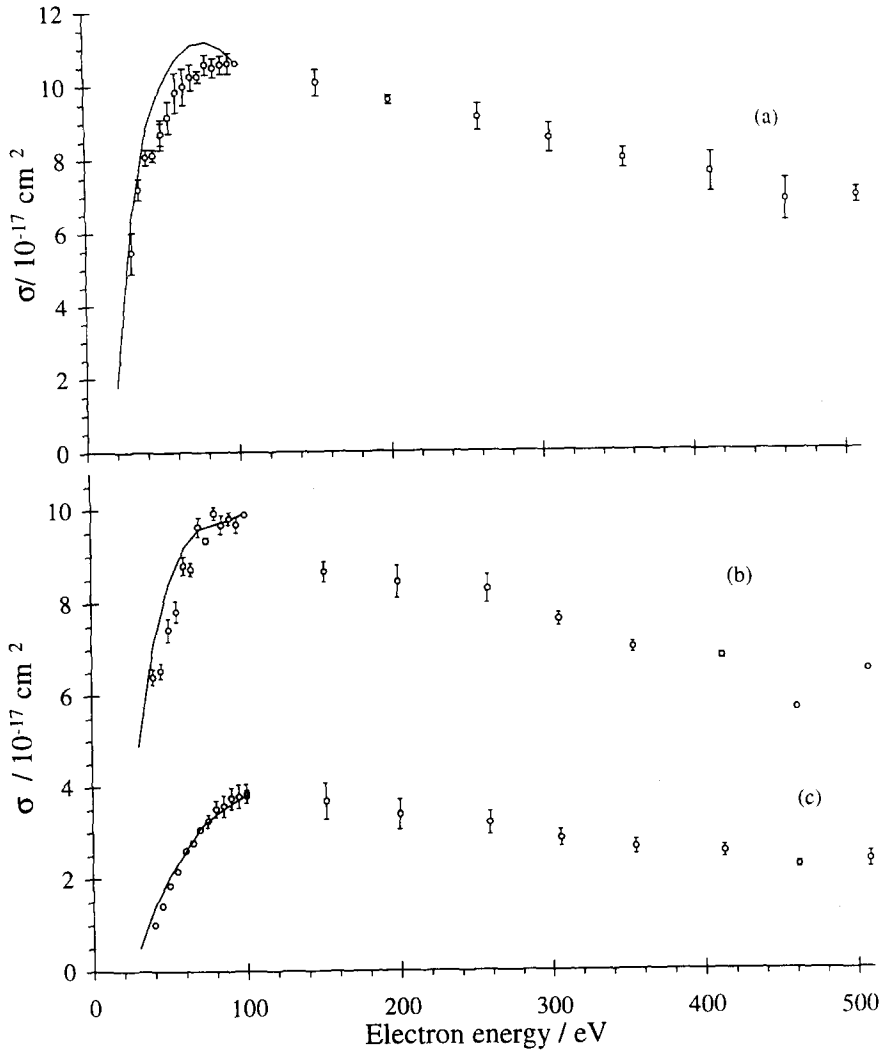

Fig. 3. Partial ionization cross-sections for forming (a) O_3^+ (b) O_2^+ and (c) O^+ from ozone. The values determined in this work are marked as circles (○) whilst the values from the only previous study [8] are joined with a line. The error bars on the values determined in this study represent two standard deviations, and are only shown when large enough to be clear in the figure.

the adjacent values reproduced this feature, as evidenced by the small standard deviations of these points (Table 1).

The data analysis procedure described above uses only the ozone partial ionization cross-sections for the formation of O_3^+ and O_2^+ at 100 eV from the literature to derive the composition of our ozone sample (Eq. (8)), and no literature cross-sections for the formation of O^+ are involved. Hence, the fact that our values for $\sigma_{O_3}^{D''}(E)$ agree closely with the previous determination below 100 eV both validates the data analysis procedure described above and shows that the deconvolution of the signals due to ionization of O_2 in the previous work using the modulated gas beam [8] was satisfactory.

As discussed above, our experimental arrangement will strongly discriminate against fragment ions with significant (> 1 eV) kinetic

Table 1
Partial electron ionization cross-sections for forming the indicated product ion from ozone (the numbers in parentheses indicate the standard deviation in the last figure of each cross-section)

Incident electron energy (eV)	Partial ionization cross-section (10^{-17} cm^2)		
	O_3^+	O_2^+	O^+
40	8.08(21)	6.39(17)	1.00(07)
45	8.12	6.53(16)	1.41(04)
50	8.72(30)	7.42(23)	1.84(08)
55	9.17(43)	7.81(20)	2.15(08)
60	9.82(54)	8.79(17)	2.59(12)
65	9.97(49)	8.71(13)	2.76(10)
70	10.23(35)	9.63(18)	3.05(20)
75	10.25(16)	9.34(08)	3.24(13)
80	10.58(27)	9.92(13)	3.49(18)
85	10.50(26)	9.67(18)	3.56(22)
90	10.57(25)	9.80(12)	3.73(23)
95	10.58(28)	9.68(18)	3.77(24)
100	10.60[a]	9.90[a]	3.78(14)
152	10.07(36)	8.66(19)	3.65(37)
200	9.59(11)	8.44(31)	3.34(31)
259	9.11(36)	8.27(28)	3.14(23)
306	8.54(40)	7.61(12)	2.81(16)
355	7.97(27)	7.00(11)	2.60(14)
413	7.57(54)	6.79(10)	2.50(11)
462	6.82(58)	5.65(04)	2.21(11)
509	6.90(21)	6.49(05)	2.31(16)

[a] Values set by normalization procedure. See text for details.

energies. Hence the cross-sections reported in this work will not contain a contribution due to double and higher forms of ionization, and should be rigorously described as partial single ionization cross-sections. However, coincidence experiments carried out in this laboratory indicate that the dissociative double ionization cross-section of O_3 is significantly smaller than that for both CS_2 and OCS [24], and hence we feel that including the contribution of multiple ionization would not affect the values reported within their error limits.

6. Conclusions

We have developed a data analysis procedure to separate the contributions of molecular oxygen and ozone to the O^+ and O_2^+ signals in a time-of-flight mass spectrum, and used that procedure to extract the partial ionization cross-sections of ozone from a series of mass spectra of an O_2/O_3 mixture from 40 to 500 eV. Below 100 eV, where data are available, these values are in good agreement with their sole previous determination [8].

Acknowledgements

These experiments were made possible by the financial support of the Nuffield Foundation (S.D.P.) the Central Research Fund of the University of London (S.D.P.), the Graduate School of University College London (S.D.P.) and the Royal Society (N.J.M.). K.A.N. thanks the EPSRC for a research studentship.

References

[1] J.I. Steinfeld, S.M. Alder-Golden and J.W. Gallagher, J. Phys. Chem. Ref. Data, 16 (1987) 911.
[2] M. Horvath, L. Bilitzky and J. Huttner, in R.J.H. Clark (Ed.), Topics in Inorganic Chemistry, Val. 20, 1985.
[3] Y. Okamoto and Y. Itikawa, Chem. Phys. Lett., 203 (1993) 61.
[4] K.N. Joshipura, Pramana, 32 (1989) 139.
[5] K.N. Joshipura, Indian J. Pure App. Phys., 23 (1986) 525.
[6] J.A. Davies, W.M. Johnstone, N.J. Mason, P. Biggs and R.P. Wayne, J. Phys. B, 26 (1993) L767.
[7] T.W. Shyn and C.J. Sweeny, Phys. Rev. A, 47 (1993) 2919.
[8] M.W. Siegel, Int. J. Mass Spectrom. Ion Phys., 44 (1982) 19.
[9] D. Mehandjiev and A. Naidenov, Ozone Sci. Eng., 14 (1983) 277.
[10] W.M. Johnstone, N.J. Mason, W.R. Newell, P. Biggs, G. Marston and R.P. Wayne, J. Phys. B, 25 (1992) 3873.
[11] W.C. Wiley and I.H. McLaren, Rev. Sci. Instrum., 26 (19955) 1150.
[12] E. Krishnakumar and S.K. Srivastava, J. Phys. B, 21 (1988) 1055.
[13] M.R. Bruce and R.A. Bonham, Z. Phys. D, 24 (1992) 149.
[14] B. Van Zyl and T.M. Stephen, Phys. Rev. A, 50 (1994) 3164.
[15] R. Locht, G. Hagenow, K. Hottmann and H. Baumgartel, Chem. Phys., 151 (1991) 137.
[16] M.V.V.S. Rao and S.K. Srivastava J. Geophys. Res., 96 (1991) 17563.
[17] E. Mark, T.D. Mark, Y.B. Kim and K. Stephan, J. Chem. Phys., 75 (1981) 4446.

[18] D.M. Curtis and J.H.D. Eland Int. J. Mass Spectrom. Ion Process 63 (1985) 241.
[19] R. Locht, J. Schopman, H. Wankenne and J. Momigny, Chem. Phys., 7 (1975) 393.
[20] Y. Itikawa, M. Hayashi, A. Ichimura,K. Onda, K. Sakimoto, K. Takayanagi, M. Nakimura, H. Nishimura and T. Takayanagi, J. Phys. Chem. Ref. Data, 15 (1986) 985.
[21] P.B. Armentrout, S.M. Tarr, A. Sori and R.S. Freund, J. Chem. Phys., 75 (1981) 2786.
[22] Y. Itikawa, A. Ichimura, K. Onda, K. Sakimoto, K. Takayanagi, Y. Hatano, M. Hayashi, H. Nishimura and S. Tsurubuchi, J. Phys. Chem. Ref. Data, 18 (1989) 23.
[23] R.P. Wayne, P. Biggs and G. Marston, personal communication, 1995.
[24] K.A. Newson and S.D. Price, in preparation.